

# THE GPD PROGRAM AT COMPASS

A. Sandacz

*on behalf of the COMPASS collaboration*

*National Centre for Nuclear Research, Warsaw, Poland*

*E-mail: sandacz@fuw.edu.pl*

## Abstract

The high energy polarised muon beam available at CERN, with positive or negative charge, make COMPASS a unique place for GPD studies. The COMPASS program of GPD studies is reviewed and various observables for this program and expected accuracies are discussed. The necessary developments of the experimental setup and the first results of the test runs are also presented.

## 1 Introduction

Generalised Parton Distributions (GPDs) [1–3] contain a wealth of information on the partonic structure of the nucleon. In particular, they allow a novel description of the nucleon as an extended object, sometimes referred to as 3-dimensional ‘nucleon tomography’ [4]. GPDs also allow access to such a fundamental property of the nucleon as the orbital angular momentum of quarks [2]. For reviews of the GPDs see Refs [5–7].

The mapping of the nucleon GPDs requires comprehensive experimental studies of hard processes, Deeply Virtual Compton Scattering and Hard Exclusive Meson Production, in a broad kinematic range. In the future program [8] we propose to measure both DVCS and HEMP using an unpolarised proton target during a first period, in order to constrain mainly GPD  $H$ , and a transversely polarised ammonia target during another period in order to constrain the GPD  $E$ .

## 2 The proposed setup

The COMPASS apparatus is located at the high-energy (100-200 GeV) and highly-polarized  $\mu^\pm$  beam line of the CERN SPS. At present it consists of a two-stage spectrometer comprising various tracking detectors, electromagnetic and hadron calorimeters, and particle identification detectors grouped around 2 dipole magnets SM1 and SM2 in conjunction with a longitudinally or transversely polarized target. By installing a recoil proton detector (RPD) around the target to ensure exclusivity of the DVCS and HEMP events, COMPASS could be converted into a facility measuring exclusive reactions within a kinematic domain from  $x \sim 0.01$  to  $\sim 0.1$ , which cannot be explored at any other existing or planned facility in the near future. Thus COMPASS could explore the uncharted  $x$  domain between the HERA collider experiments and the fixed-target experiments as HERMES and the planned 12 GeV extension of the JLAB accelerator. For values of  $x$

below  $10^{-1}$ , the outgoing photon (or meson) is emitted at an angle below  $10^\circ$  which corresponds for the photon to the acceptance of the two existing COMPASS electromagnetic calorimeters ECAL1 and ECAL2. For charged particles such an angular range is within the acceptance of the tracking devices and the RICH detector. To access higher  $x$  values a large angular acceptance calorimeter ECAL0 is needed, which is presently under study.

The data will be collected with polarized  $\mu^+$  and  $\mu^-$  beams. Assuming in total 280 days of data taking,  $\mu^+$  beam flux of  $4.6 \cdot 10^8$   $\mu$  per SPS spill and three times smaller flux for  $\mu^-$  beam, a reasonable statistics for the DVCS process can be accumulated for  $Q^2$  values up to  $8 \text{ GeV}^2$ . It is worth noting that an increase of the number of muons per spill by a factor 4 could result in an increase in the range in  $Q^2$  up to about  $12 \text{ GeV}^2$ .

### 3 Planned measurements

The complete GPD program at COMPASS will comprise the measurements of the DVCS cross section with polarized positive and negative muon beams and at the same time the measurements of a large set of mesons ( $\rho$ ,  $\omega$ ,  $\phi$ ,  $\pi$ ,  $\eta$ , ...).

#### 3.1 Deeply Virtual Compton Scattering

DVCS is considered to be the theoretically cleanest of the experimentally accessible processes because effects of next-to-leading order and higher twist contributions are under theoretical control [9]. The competing Bethe-Heitler (BH) process, which is elastic lepton-nucleon scattering with a hard photon emitted by either the incoming or outgoing lepton, has a final state identical to that of DVCS so that both processes interfere at the level of amplitudes.

COMPASS offers the advantage to provide various kinematic domains where either BH or DVCS dominates. The collection of almost pure BH events at small  $x$  allows one to get an excellent reference yield and to control accurately the global efficiency of the apparatus. In contrast, the collection of an almost pure DVCS sample at larger  $x$  will allow the measurement of the  $x$  dependence of the  $t$ -slope of the cross section, which is related to the tomographic partonic image of the nucleon. In the intermediate domain, the DVCS contribution will be boosted by the BH process through the interference term. The dependence on  $\phi$ , the azimuthal angle between lepton scattering plane and photon production plane, is a characteristic feature of the cross section [9].

COMPASS is presently the only facility to provide polarized leptons with either charge: polarized  $\mu^+$  and  $\mu^-$  beams. Note that with muon beams one naturally reverses both charge and helicity at once. Practically  $\mu^+$  are selected with a polarisation of  $-0.8$  and  $\mu^-$  with a polarization of  $+0.8$ . The difference and sum of cross sections for  $\mu^+$  and  $\mu^-$  combined with the analysis of  $\phi$  dependence allow us to isolate the real and imaginary parts of the leading twist-2 DVCS amplitude, and of higher twist contributions.

In the following sections we show projections for DVCS measurements with an unpolarised proton target (3.1.1 and 3.1.2) and with a transversely polarised ammonia target (3.1.3). For each target the integrated muon flux was taken the same as described in Sect. 2 and the value of the global efficiency was assumed to be equal to 0.1.

### 3.1.1 $x$ -dependence of the $t$ -slope of DVCS

The  $t$ -slope parameter  $B(x)$  of the DVCS cross section  $\frac{d\sigma}{dt}(x) \propto \exp(-B(x)|t|)$  can be obtained from the beam charge and spin sum of the cross sections after integration over  $\phi$  and BH subtraction. The expected statistical accuracy of the measurements of  $B(x)$  at COMPASS is shown in Fig. 1. The upper plot corresponds to the acceptance of the existing electromagnetic calorimeters, while the lower one is obtained assuming that in addition the new calorimeter ECAL0 will be also available. The systematic errors are mainly due to uncertainties involved in the subtraction of the BH contribution. At  $x > 0.02$  they are small compared to the statistical errors. For the simulations the simple ansatz  $B(x) = B_0 + 2\alpha' \log(\frac{x_0}{x})$  was used. As neither  $B_0$  nor  $\alpha'$  are known in the COMPASS kinematics, for the simulations shown in Fig. 1 we chose the values  $B_0 = 5.83 \text{ GeV}^2$ ,  $\alpha' = 0.125$  and  $x_0 = 0.0012$ . The precise value of the  $t$ -slope parameter  $B(x)$  in the COMPASS  $x$ -range will yield new and significant information in the context of ‘nucleon tomography’ as it is expected in Ref. [10].

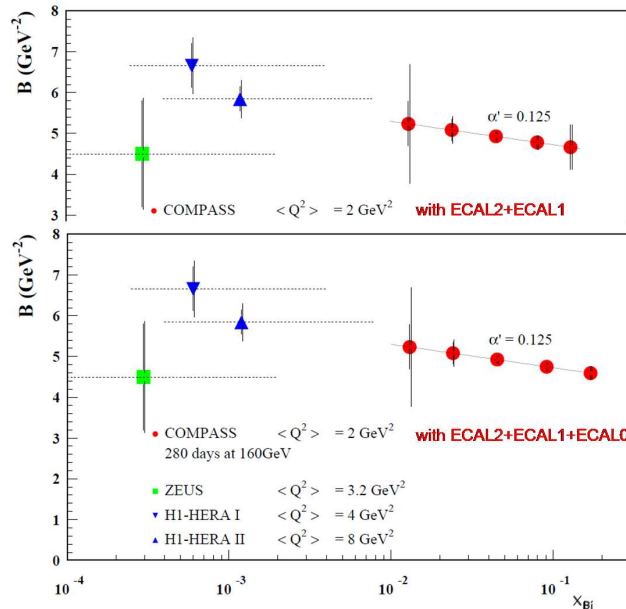


Figure 1: The  $x$  dependence of the fitted  $t$ -slope parameter  $B$  of the DVCS cross section. COMPASS projections are calculated for  $1 < Q^2 < 8 \text{ GeV}^2$  and compared to HERA results for which the mean value  $\langle Q^2 \rangle$  is in this range.

### 3.1.2 Beam charge and spin difference of cross sections

Fig. 2 shows the projected statistical accuracy for the beam charge and spin difference of cross section  $\mathcal{D}_{CS,U}$  measured as a function of  $\phi$  in a selected  $(x, Q^2)$  bin. The difference is defined as

$$\mathcal{D}_{CS,U} = d\sigma^{\leftarrow+} - d\sigma^{\rightarrow-}, \quad (1)$$

with arrows indicating the orientations of the longitudinal polarisation of the beams. The difference  $\mathcal{D}_{CS,U}$  is sensitive to the real part of the DVCS amplitude which is a convolution of GPDs with the hard scattering kernel over the whole range of longitudinal momenta of

exchanged quarks. Therefore measurements of this asymmetry provide strong constraints on the models of GPD. Two of the curves shown in the figure are calculated using the 'VGG' GPD model [11]. As this model is meant to be applied mostly in the valence region, typically the value  $\alpha' = 0.8$  is used in the 'reggeized' parameterization of the correlated  $x, t$  dependence of GPDs. For comparison also the model result for the 'factorized'  $x, t$  dependence is shown, which corresponds to  $\alpha' \approx 0.1$  in the reggeized ansatz. A recent theoretical development [12] exploiting dispersion relations for Compton form factors was successfully applied to describe DVCS observables at very small values of  $x$  typical for the HERA and extended to include DVCS data from HERMES and JLAB. The prediction for COMPASS from this analysis are shown as additional curves.

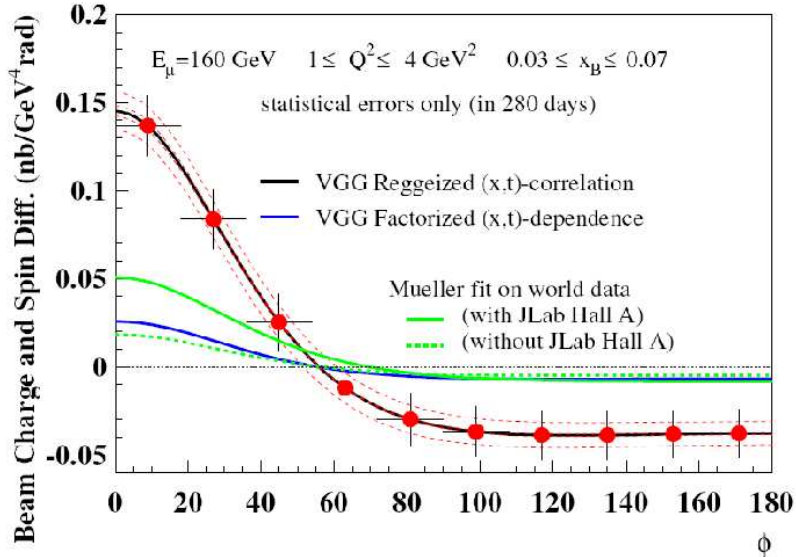


Figure 2: Projections for the beam charge and spin difference of cross sections measured at COMPASS for  $0.03 \leq x \leq 0.07$  and  $1 \leq Q^2 \leq 4 \text{ GeV}^2$ . The red and blue curves correspond to two variants of the VGG model [11] while the green curves show predictions based on the first fits to the world data [12].

As the overall expected data set from the GPD program for COMPASS will allow 9 bins in  $x$  vs.  $Q^2$ , each of them expected to contain statistics sufficient for stable fits of the  $\phi$  dependence, a determination of the 2-dimensional  $x, Q^2$  (or  $x, t$ ) dependence will be possible for the various Fourier expansion coefficients  $c_n$  and  $s_n$  [9], thereby yielding information on the nucleon structure in terms of GPDs over a range in  $x$ . These data are expected to be very useful for future developments of reliable GPD models able to simultaneously describe the *full*  $x$ -range.

### 3.1.3 Predictions for the transverse target spin asymmetry

Transverse target spin asymmetries for exclusive photon production are important observables for studies of the GPD  $E$ , and for the determination of the role of the orbital momentum of quarks in the spin budget of the nucleon. The sensitivity of these asymmetries to the total angular momentum of  $u$  quarks,  $J_u$ , was estimated for the transversely polarised protons in a model dependent way in Ref. [13].

The transverse target spin asymmetries for the proton will be measured with the transversely polarised ammonia target, similar to the one used at present by COMPASS. Two options are considered for the configuration of the target magnet and the RPD, each with a different impact on the range of measurable energy of the recoil proton.

The transverse spin dependent part of the cross sections will be obtained by subtracting the data with opposite values of the azimuthal angle  $\phi_s$ , which is the angle between the lepton scattering plane and the target spin vector. In order to disentangle the  $|DVCS|^2$  and the interference terms with the same azimuthal dependence, it is necessary to take data with both  $\mu^+$  and  $\mu^-$  beams, because only in the difference and the sum of  $\mu^+$  and  $\mu^-$  cross sections these terms become separated. Both asymmetries for the difference and the sum of  $\mu^+$  and  $\mu^-$  of transverse spin dependent cross sections will be analysed. The difference (sum) asymmetry  $A_{CS,T}^D$  ( $A_{CS,T}^S$ ) is defined as the ratio of the  $\mu^+$  and  $\mu^-$  cross section difference (sum) divided by the lepton charge-averaged, unpolarised cross section. Here  $CS$  indicates that both lepton charge and lepton spin are reversed between  $\mu^+$  and  $\mu^-$ , and  $T$  is for the transverse target polarisation.

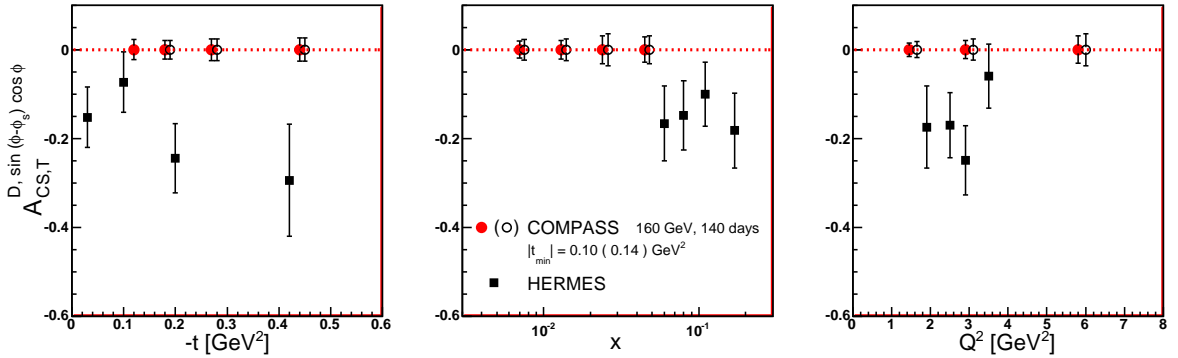


Figure 3: The expected statistical accuracy of  $A_{CS,T}^{D, \sin(\phi - \phi_s) \cos \phi}$  as a function of  $-t$ ,  $x$  and  $Q^2$ . Solid and open circles correspond to the simulations for the two considered configurations of the target region. Also shown is the asymmetry  $A_{UT}^{\sin(\phi - \phi_s) \cos \phi}$  measured by HERMES [13] with its statistical errors.

As an example, the results from the simulations of the expected statistical accuracy of the asymmetry  $A_{CS,T}^{D, \sin(\phi - \phi_s) \cos \phi}$  are shown in Fig. 3 as a function of  $-t$ ,  $x$  and  $Q^2$  for the two considered configurations of the target region. Here  $\sin(\phi - \phi_s) \cos \phi$  indicates the type of azimuthal modulations. This asymmetry is an analogue of the asymmetry  $A_{UT}^{\sin(\phi - \phi_s) \cos \phi}$  measured by HERMES with unpolarised electrons, also shown in the figure. Typical values of the statistical errors of  $A_{CS,T}^{D, \sin(\phi - \phi_s) \cos \phi}$ , as well as of the seven remaining asymmetries related to the twist-2 terms in the cross section, are expected to be  $\approx 0.03$ .

### 3.2 Hard Exclusive Meson Production

Hard exclusive vector meson production is complementary to DVCS as it provides access to various other combinations of GPDs. For vector meson production only GPDs  $H$  and  $E$  contribute, while for pseudoscalar mesons GPDs  $\tilde{H}$  and  $\tilde{E}$  play a role. We recall that DVCS depends on the four GPDs. Also in contrast to DVCS, where gluon contributions enter only beyond leading order in  $\alpha_s$ , in HEMP both quark and gluon

GPDs contribute at the same order. For example

$$H_{\rho^0} = \frac{1}{\sqrt{2}}\left(\frac{2}{3}H^u + \frac{1}{3}H^d + \frac{3}{8}H^g\right), \quad H_\omega = \frac{1}{\sqrt{2}}\left(\frac{2}{3}H^u - \frac{1}{3}H^d + \frac{1}{8}H^g\right), \quad H_\phi = -\frac{1}{3}H^s - \frac{1}{8}H^g.$$

Therefore by combining the results for various mesons the GPDs for various quark flavours and for gluons could be disentangled.

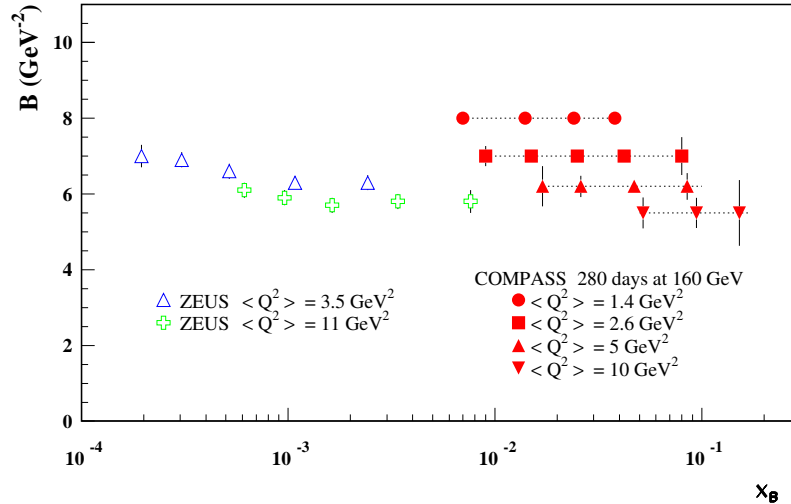


Figure 4: Projections for measuring the  $t$ -slope parameter  $B$  in exclusive  $\rho^0$  production, calculated for  $1 \geq Q^2 \geq 20 \text{ GeV}^2$  compared to ZUES results with similar  $\langle Q^2 \rangle$ . Only statistical errors are shown.

Data on exclusive production of vector mesons production, which will be recorded simultaneously to the DVCS measurements, will be used to determine corresponding cross sections and  $t$ -slope parameters  $B(x)$ . As an example, in Fig. 4 we show projections for the  $\rho^0$  meson. The simulations are based on a model developed for COMPASS, where the  $Q^2$  and  $\nu$  dependences are taken from the parameterisation of the NMC data and the absolute normalisation is obtained using predictions of Ref. [14]. The statistical precision expected for 280 days at 160 GeV muon beam energy is shown for different bins of  $x$  and  $Q^2$ . The data from ZEUS, which cover a lower  $x$  range are also shown for comparison. The projections for COMPASS include a dependence of the slope  $B$  on  $Q^2$ , as observed in both ZEUS and H1 experiments, but no correlation between the slope value and  $x$  was assumed here.

It was pointed out that vector meson production on a transversely polarised target is sensitive to the nucleon helicity-flip GPD  $E$  [5, 15]. This GPD offers unique views on the orbital angular momentum carried by partons in the proton [2] and on the correlation between polarisation and spatial distribution of partons [4]. The azimuthal asymmetry  $A_{UT}^{\sin(\phi-\phi_s)}$  for exclusive production of a vector meson off a transversely polarised nucleon depends linearly on the GPD  $E$  and at COMPASS kinematic domain it can be expressed as

$$A_{UT}^{\sin(\phi-\phi_s)} \sim \sqrt{t_0 - t} \frac{\text{Im}(\mathcal{E}^M \mathcal{H}_M^*)}{|\mathcal{H}_M|^2}, \quad (2)$$

where  $t_0$  is the minimal momentum transfer. The quantities  $\mathcal{H}_M$  and  $\mathcal{E}_M$  are weighted sums of convolutions of the GPD  $H^{q,g}$  and  $E^{q,g}$ , respectively, with the generalised distribution amplitude (GDA) of the produced meson and a hard scattering kernel [5]. The

weights depend on the contributions of quarks of various flavours and of gluons to the production of meson  $M$ .

We note that the production of  $\rho$ ,  $\omega$ ,  $\phi$  vector mesons is already being investigated at COMPASS [16]. The preliminary results from COMPASS on the transverse target spin asymmetries for  $\rho^0$  production off transversely polarised protons and deuterons were presented at this conference [17].

## 4 Validation tests and outlook

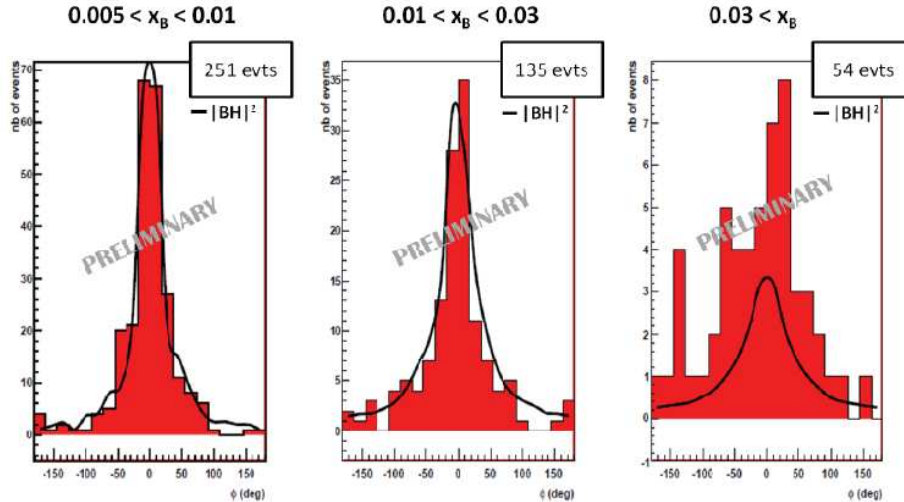


Figure 5: The distribution of the azimuthal angle  $\phi$  for observed exclusive single photon production measured in the 2009 DVCS test run at COMPASS. The lines represent the expected BH event yield.

The setup used in 2008 and 2009 for the meson spectroscopy measurements with hadron beams happens to be an excellent *prototype* to perform validation measurements for DVCS. A first measurements of exclusive  $\gamma$  production on a 40 cm long LH target, with detection of the slow recoiling proton in the RPD have been performed during short test runs in 2008 and 2009 using 160 GeV  $\mu^+$  and  $\mu^-$  beams. They were performed with the present hadron setup, all the standard COMPASS tracking detectors, the ECAL1 and ECAL2 electromagnetic calorimeters for photon detection and appropriate triggers. An efficient selection of single photon events, and suppression of the background is possible by using the combined information from the forward COMPASS detectors and the RPD.

A way to identify the observed process,  $\mu + p \rightarrow \mu' + \gamma + p'$ , to which both the DVCS and Bethe-Heitler process contribute, is to look at the angle  $\phi$  between the leptonic and hadronic planes. The observed distributions, after applying all cuts and selections and for  $Q^2 > 1$  (GeV/c)<sup>2</sup>, are displayed in Fig. 5 and compared to the predictions from the Monte Carlo simulations for the BH event yield. The Bethe-Heitler contribution shows a characteristic peak at  $\phi \simeq 0$ . The overall detection efficiency can be deduced from the relative normalization of the two distributions for the low  $x$ -region dominated by BH. The global efficiency is equal to  $0.14 \pm 0.05$  in agreement with the value 0.1 assumed for the proposal [8].

The proposal to extend the physics program of COMPASS, including the GPD studies, was approved at CERN in 2010. A possible start of the GPD program, first with a 2.5 m long liquid hydrogen target, is planned for 2012. A few weeks run with the muon beam will be devoted to the commissioning of a 4 m long RPD being presently constructed, and of a central part (20%) of ECAL0, which will be available in 2012. It will be followed by a short physics run with an objective to measure  $t$ -slope for DVCS.

## References

- [1] D. Mueller *et al*, Fortsch. Phys. **42** (1994) 101.
- [2] X. Ji, Phys. Rev. Lett. **78** (1997) 610; Phys. Rev. D **55** (1997) 7114.
- [3] A.V. Radyushkin, Phys. Lett. B **385** (1996) 333; Phys. Rev. D **56** (1997) 5524.
- [4] M. Burkardt, Phys. Rev. D **62** (2000) 071503; erratum-ibid. D **66** (2002) 119903; Int. J. Mod. Phys. A **18** (2003) 173; Phys. Lett. B **595** (2004) 245.
- [5] K. Goeke, M.V. Polyakov and M. Vanderhaegen, Prog. Part. in Nucl. Phys. **47** (2001) 401.
- [6] M. Diehl, *Generalized Parton Distributions*, DESY-thesis-2003-018, hep-ph/0307382.
- [7] A.V. Belitsky and A.V.Radyushkin, Phys. Rep. **418** (2005) 1.
- [8] The COMPASS Collaboration, *COMPASS-II Proposal*, CERN-SPSC-2010-014, SPSC-P-340, May 17, 2010.
- [9] A.V. Belitsky, D. Müller and A. Kirchner, Nucl. Phys. **B 629** (2002) 323.
- [10] M. Strikman and C. Weiss, Phys. Rev. **D69** (2004) 054012.
- [11] M. Vanderhaeghen, P.A.M. Guichon and M. Guidal, Phys. Rev. Lett. **80** (1998) 5064; Phys. Rev. D **60** (1999) 094017;
- [12] K. Kumericki and D. Mueller, hep-ph/0904.0458.
- [13] A. Airapetian *et al*, JHEP **06** (2008) 066.
- [14] S. Goloskokov and P. Kroll, Eur. Phys. J. C **53** (2008) 367.
- [15] F. Ellinghaus, W.-D. Nowak, A.V. Vinnikov, and Z. Ye, Eur. Phys. J. **C46** 729 (2006), hep-ph/0506264.
- [16] A. Sandacz, *Exclusive processes in leptonproduction at COMPASS*, in Proceedings of the International Conference on the Structure and the Interactions of the Photon, PHOTON09, Hamburg, 2009, ed. O. Behnke *et al*, Verlag Deutsches Elektronen-Synchrotron, Hamburg, 2010, p. 294.
- [17] P. Sznajder, this conference.